SIMULATION AND OPTIMIZATION OF THE SEED METERING PLATE FOR AN AIR-SUCTION PRECISION SEED METERING DEVICE WITH MULTIPLE-SEED-PER-HILL BASED ON CFD

/

基于 CFD 的一穴多粒气吸式精密排种器排种盘仿真与优化

Zhiwei WANG[1)], Yanwu JIANG[1)], Deyi ZHANG[1)], Sugirbay ADILET[2)], Naishuo WEI[1)], Jianguo ZHOU[1)], Jun CHEN[1*)]

[1)] College of Mechanical and Electronic Engineering, Northwest A&F University, Yangling, Shaanxi, 712100, China

[2)] Research School of Veterinary Medicine and Agriculture, Shakarim University, Semey 071400, Kazakhstan

** Corresponding author: Jun Chen. E-mail address: chenjun_jdxy@nwsuaf.edu.cn*

DOI: https://doi.org/10.35633/inmateh-79-02

***Keywords:** Small-seed crops, Pneumatic adsorption, Hill-drop sowing, Suction-hole pressure, Airflow-field mapping, Parameter optimization*

ABSTRACT

To enhance the seeding accuracy of multi-seed-per-hole operations for small-seed crops, a combined experimental-CFD optimization method for an air-suction seed metering plate was developed. Single-factor tests established that the suitable suction-hole diameter was 0.4-0.6 times the equivalent seed diameter, and threshold-based negative-pressure tests were used to define the acceptable suction-hole negative-pressure range for millet, broomcorn millet, and rapeseed. CFD pressure-tracing analysis was then performed to quantify the mapping between suction-hole pressure and air-chamber inlet negative pressure. On this basis, a three-factor, three-level optimization test was conducted using inlet negative pressure, suction-hole diameter, and suction-hole thickness as variables, with the qualification rate of suction-hole pressure as the response. The optimized parameter combinations were 2.51 kPa, 0.88 mm, and 0.31 mm for millet; 2.97 kPa, 1.12 mm, and 0.35 mm for broomcorn millet; and 2.35 kPa, 0.93 mm, and 0.32 mm for rapeseed. Bench validation showed seed-filling rates of 93%, 97%, and 96%, respectively. The results demonstrate that the proposed method can effectively reduce empirical trial workload and provide a practical basis for the design of pneumatic precision seed metering plates for small-seed crops.

摘要

为提高小籽粒作物一穴多粒作业的播种精度，本文提出了一种针对气吸式排种盘的 CFD 仿真试验联合优化方法。通过单因素试验确定，适宜的吸孔直径应为种子当量直径的 0.4～0.6 倍；同时，基于基准压力试验界定了谷子、糜子和油菜籽适宜的吸孔负压范围。随后，采用 CFD 压力追踪分析方法，定量建立了吸孔负压与气室入口负压之间的映射关系。在此基础上，以入口负压、吸孔直径和吸孔厚度为试验因素，以吸孔负压合格率为响应指标，开展了三因素三水平优化试验。优化结果表明：谷子的最优参数组合为 2.51 kPa、0.88 mm 和 0.31 mm；糜子的最优参数组合为 2.97 kPa、1.12 mm 和 0.35 mm；油菜籽的最优参数组合为 2.35 kPa、0.93 mm 和 0.32 mm。台架验证结果显示，三者的充种率分别达到 93%、97%和 96%。结果表明，所提出的方法能够有效减少经验试验工作量，并可为小籽粒作物气力式精密排种盘的设计提供实用依据。

INTRODUCTION

Millet, broomcorn millet, and rapeseed are important economic crops in Northwest China, where sowing practices include manual broadcasting, drill sowing, and hill-drop sowing, while the level of mechanization in some mountainous and hilly areas remains relatively low *(Cong et al., 2014; Gao et al., 2022; Cao et al., 2026)*. The regional climate is characterized by low temperature, aridity, and limited precipitation, which are unfavorable for seed germination and early growth. Consequently, plastic-film mulching and multi-seed-per-hole sowing are commonly adopted to improve seedling establishment. Under these agronomic conditions, single-seed precision sowing is generally unsuitable for small-seed crops.

Precision sowing technology can significantly improve sowing quality by placing a controlled number of seeds at specified row spacing, plant spacing, and sowing depth, while simultaneously completing operations such as fertilization, soil compaction, and mulching *(Gao et al., 2026; Wei et al., 2026)*. The seed metering device is the core component of precision sowing systems and can be broadly classified into mechanical and pneumatic types *(Gaikwad and Sirohi, 2008; Karayel et al., 2022; Bustos-Gaytán et al., 2025)*.

Among them, pneumatic seed metering devices are widely used because of their strong adaptability to seed-size variation, low mechanical damage, and suitability for relatively high-speed operation *(Wang et al., 2017; Li et al., 2023; Yang et al., 2026)*.

Previous studies have shown that vacuum pressure, hole geometry, plate speed, and seed delivery conditions jointly determine the performance of precision seeders *(Ibrahim et al., 2018; Rezaei Asl et al., 2019)*. *Karayel et al. (2004)* mathematically analyzed the vacuum-pressure requirement of a precision seeder, *Yazgi and Degirmencioglu (2007)* optimized seed-spacing uniformity through response surface methodology, *Panning et al. (2000)* evaluated laboratory and field methods for planter spacing assessment, and *Onal et al. (2012)* examined the theoretical and experimental accuracy of a vacuum-type precision metering unit. In China, related studies have further improved seed filling by using dual-chamber structures, grooved-tooth disturbance, wedge-shaped agitation, and protrusion-assisted seed plates *(Ding et al., 2018; Li et al., 2019; Wang et al., 2019; Xing et al., 2020)*. However, most available studies focus on single-seed precision sowing or general spacing performance, whereas the coupled pressure-matching problem of small seeds under multi-seed-per-hole conditions remains insufficiently clarified.

Accordingly, the novelty of this study lies in three aspects: (1) an engineering matching rule between seed size and suction-hole diameter was established for small-seed multi-seed-per-hole sowing; (2) the mapping between suction-hole pressure and air-chamber inlet pressure was quantified through CFD-assisted pressure tracing; and (3) the coupled effects of inlet negative pressure, suction-hole diameter, and suction-hole thickness were optimized and validated experimentally for three representative small-seed crops. These results provide a more directly applicable design route for pneumatic seed metering plates than empirical parameter selection alone.

MATERIAL AND METHODS

Selection of suction hole diameter range

The geometry of suction holes, including shape, diameter, and thickness, plays a critical role in the performance of seed metering plates *(Dun et al., 2019; Gao et al., 2022; Ren et al., 2024)*. Considering the seed cleaning and unloading mechanisms employed in this study, concave–convex hole structures were excluded due to their incompatibility with the operational requirements.

To determine the appropriate suction hole diameter range, three types of seeds—millet, broomcorn millet, and rapeseed—were matched with a series of hole diameters ranging from 0.3 mm to 2.0 mm at intervals of 0.1 mm. The holes were fabricated using laser cutting on a steel plate with a thickness of 0.5 mm.

To ensure stable seed adsorption and transport while avoiding excessive cleaning and seed damage during release, a geometric matching method was adopted. Seeds were placed on suction holes of varying diameters, and the interaction between seed geometry and hole size was evaluated. The criterion for suitable matching was defined as the condition at which the seed just began to enter the suction hole without falling through.

Based on repeated observations and statistical screening, the relationship between suction-hole diameter and equivalent seed diameter was expressed as:

$$d_k = (0.4 - 0.6)\ d_z \tag{1}$$

where: d_k – the diameter of the seed metering plate suction hole, mm; d_z - the equivalent diameter of small-seed crops, mm.

Table 1

Range of suction hole diameters for different seed types

Item	Millet	Broomcorn millet	Rapeseed
Equivalent diameter [mm]	1.5717	2.5290	2.1331
Suction hole diameter [mm]	0.629-0.943	1.012-1.517	0.853-1.280
Median suction hole diameter [mm]	0.786	1.265	1.067

This empirical relationship is consistent with the geometric compatibility requirements between seed size and suction hole diameter, ensuring stable adsorption without multiple seed pickup. Accordingly, the suitable ranges of suction hole diameters for each seed type were determined, as summarized in Table 1. It can be observed that the suction hole diameter increases proportionally with seed size, which is consistent with the relationship $d_k = (0.4–0.6)d_z$.

Selection of negative pressure range

The negative pressure at the suction hole is a key parameter governing seed adsorption, transport, and release in pneumatic seed metering devices *(Hu et al., 2025; Shi et al., 2025)*. An appropriate negative pressure range should ensure stable seed pickup, prevent excessive seed removal during cleaning, and allow reliable seed release.

To determine the feasible range of suction hole negative pressure, a threshold-based experimental method was employed. Two types of brushes were used to simulate external disturbances during the seed cleaning process: a soft nylon brush (bristle diameter 0.09 mm) and a stiff bristle brush (diameter 0.20 mm). The lower limit of negative pressure was defined as the minimum pressure at which the seed remained attached to the suction hole when lightly contacted by the soft brush. The upper limit was defined as the pressure at which the seed was just removed when subjected to the stiff brush. Each measurement was repeated 20 times, and the average values were used to reduce experimental uncertainty. The difference between these two thresholds was taken as the effective negative pressure range for seed adsorption. This range ensures sufficient holding force during seed transport while avoiding excessive adhesion that may hinder seed release.

The experimental setup is shown in Fig. 1 and mainly consisted of a fixed frame, a PVC suction tube with a diameter of 6 mm, a vacuum pump (OL 750 AD, rated suction capacity 125 L/min), a pressure-regulating device (IRV 20-C06, adjustment range -0.5 to -100.0 kPa), and the corresponding power supplies. During the experiment, the suction tube was sealed to the back side of a single suction hole to eliminate air leakage, and the negative pressure was increased stepwise by 0.1 kPa from an initial value of -0.1 kPa until the defined threshold conditions were reached.

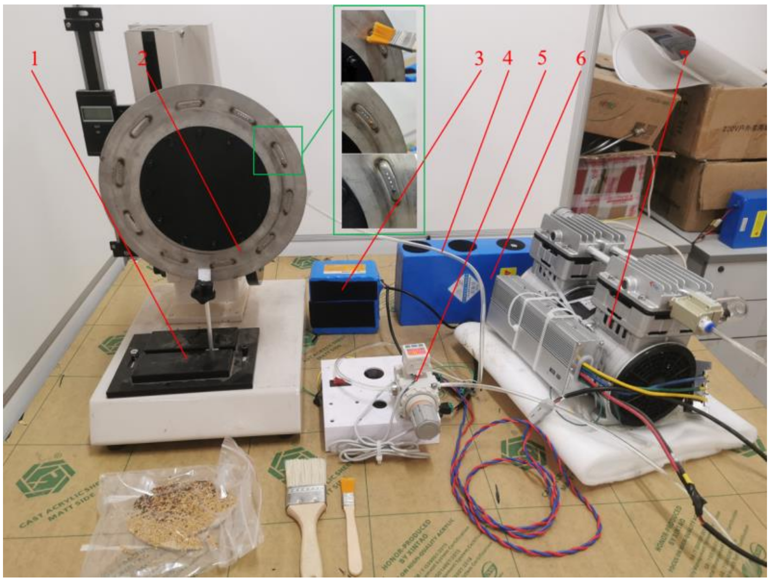

Fig. 1 - Experimental setup for the single-factor test of the seed metering plate

1. seed plate support frame; 2. seed metering plate; 3. 24V power supply for the pressure regulator; 4. suction tube; 5. pressure regulating device; 6. 36V power supply for the vacuum pump; 7. vacuum pump

As shown in Table 2, the effective negative-pressure ranges for millet, broomcorn millet, and rapeseed were 0.77-2.67 kPa, 0.97-3.25 kPa, and 0.92-2.81 kPa, respectively. Although only 0.22, 0.31, and 0.27 kPa were sufficient for the initial adsorption of the three seeds at the median suction-hole diameters, these values were below the engineering working range defined by the brushing-threshold criterion and therefore were not used for subsequent optimization.

Table 2

Range of suction hole negative pressure for different seed types

Item	Millet	Broomcorn millet	Rapeseed
Median suction hole diameter [mm]	0.8	1.2	1.0
Suction hole negative pressure range [kPa]	0.77-2.67	0.97-3.25	0.92-2.81
Median suction hole negative pressure [kPa]	1.72	2.11	1.87

Potential sources of experimental variation in the negative-pressure tests included seed-size dispersion after grading, manual differences during brush contact, the 0.1 kPa pressure-setting resolution, and local sealing variability between the suction tube and the plate. These effects were reduced by seed grading, repeated measurements, and the use of averaged values in all subsequent analyses. The obtained pressure ranges therefore provide a practical basis for balancing seed retention and release during pneumatic metering.

Simulation-based determination of air chamber suction inlet pressure range

To establish the relationship between the air-chamber inlet negative pressure and the suction-hole pressure of the seed metering plate, CFD simulations were conducted on the airflow field within the chamber.

As shown in Fig. 2, a three-dimensional model of the air chamber was developed in SolidWorks and imported into ANSYS Fluent for numerical simulation. Considering the circumferential symmetry of the chamber around the central axis of the suction inlet, a symmetric cross-sectional model was used to reduce computational cost while retaining the dominant pressure-transfer characteristics relevant to the present study *(Zhang et al., 2022; Zhao et al., 2023; Zhong et al., 2024)*.

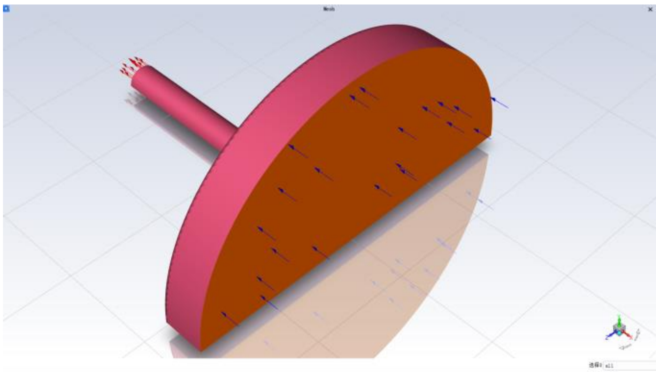

Fig. 2 - 3D model of air chamber flow field

As shown in Fig. 3, a two-dimensional symmetric cross-sectional model extracted from the 3D geometry was used for the CFD calculations. To improve the accuracy of pressure extraction, the cross-sectional model shown in Fig. 3(b) was discretized using a hexagonal-dominant cell, with local refinement applied in the suction inlet passage and suction-hole region, where the pressure gradient changed markedly. The global mesh size was approximately 0.20 mm, while the local mesh size in the refined region was reduced to 0.05 mm. Three mesh schemes were tested for mesh-independence analysis, containing approximately 28,436, 46,912, and 71,385 cells, respectively. The average pressure at three monitoring points near the suction-hole outlet was used as the mesh-independence criterion. When the number of cells increased from 46,912 to 71,385, the relative deviation of the monitored pressure was only 0.84%, indicating that further mesh refinement had a negligible effect on the simulation results. Therefore, considering both computational cost and numerical accuracy, the mesh with 46,912 cells was adopted for the subsequent simulations.

Millet was selected as the representative case for the pressure-tracing analysis. The suction inlet diameter was 30 mm, the suction-hole diameter was 0.8 mm, and the hole thickness was 0.5 mm. Three monitoring points were arranged near the suction-hole outlet, three monitoring points were arranged symmetrically near the suction-hole outlet, and their average pressure was used as the evaluation index. The inlet negative pressure was increased stepwise by 0.1 kPa.

In the simulations, air was treated as an incompressible fluid under steady turbulent flow conditions. Because the airflow inside the chamber was mainly characterized by internal negative-pressure flow, and the objective of this study was to determine the pressure-transfer relationship between the chamber inlet and the suction hole rather than to capture transient vortex evolution, the standard k–ε turbulence model was selected. Compared with more complex turbulence models, the standard k–ε model provides better numerical robustness and computational efficiency for steady engineering flows, and it has been widely used in airflow simulations of pneumatic seed-metering devices to achieve stable predictions of chamber pressure fields. The ambient conditions were set at 25 °C and 101 kPa *(Yu et al., 2014; Zhang et al., 2022; Tang et al., 2023; Wang et al., 2023; Zhong et al., 2024)*.

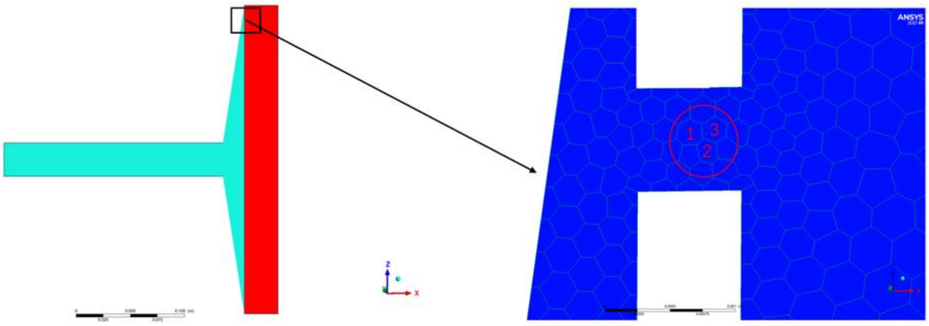

(a) (b)

Fig. 3 - Computational domain and mesh of the airflow field

(a) Geometry of the air chamber; (b) Mesh of the cross-sectional plane.

Pressure–velocity coupling was handled using the SIMPLE algorithm, and second-order discretization schemes were applied to the pressure and momentum equations. The solution was considered converged when the residuals of the continuity and momentum equations were reduced below 1×10^{-5}, and the monitored suction-hole pressure remained stable with no further noticeable variation.

Eight representative inlet-pressure conditions, namely 1.9, 2.1, 2.4, 2.7, 3.1, 3.5, 3.9, and 4.1 kPa, were extracted from the stepwise simulation process. The corresponding suction-hole pressures were 0.62, 0.74, 1.24, 1.67, 2.06, 2.25, 2.61, and 2.73 kPa, respectively.

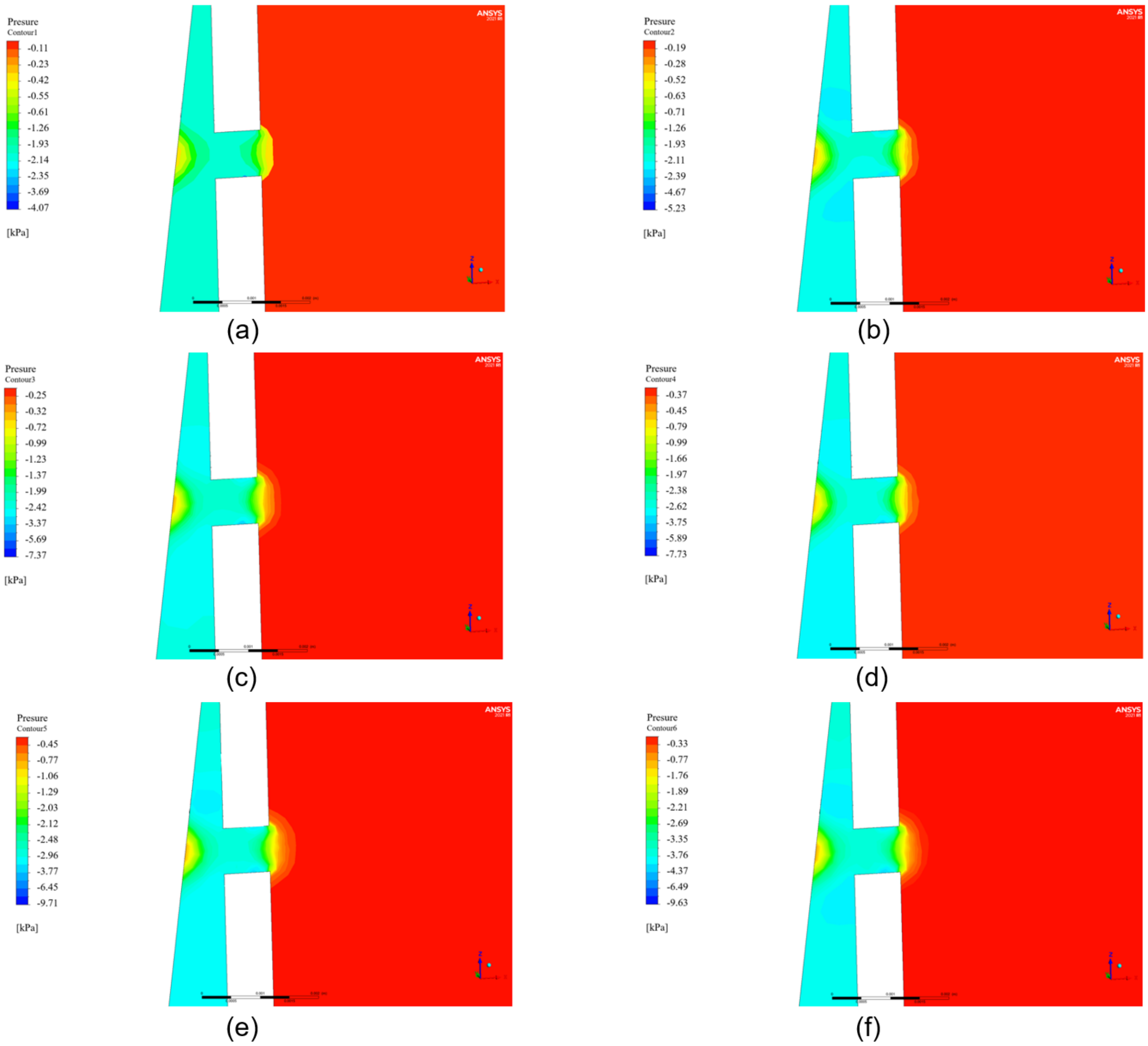

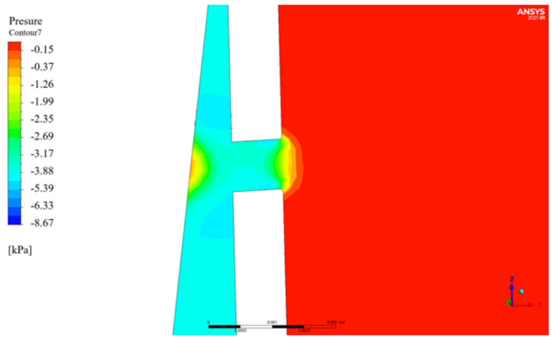

(g)

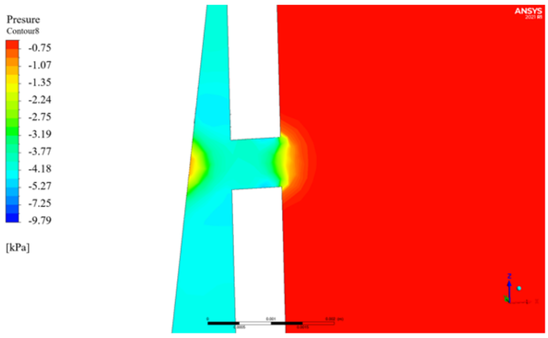

(h)

Fig. 4 - Pressure contours at suction holes under different air chamber inlet pressures

(a) 1.9 kPa; (b) 2.1 kPa; (c) 2.4 kPa; (d) 2.7 kPa; (e) 3.1 kPa; (f) 3.5 kPa; (g) 3.9 kPa; (h) 4.1 kPa

As shown in Fig. 4, the pressure contours at the suction hole changed regularly with increasing inlet negative pressure. When the chamber inlet pressure was lower than about 2.1 kPa, the suction-hole pressure was below the experimentally acceptable lower limit for millet. When the chamber inlet pressure exceeded about 3.9-4.1 kPa, the suction-hole pressure approached or exceeded the upper limit of the qualified range, indicating a risk of over-adsorption. Therefore, the corresponding inlet pressure range for millet was determined to be 2.11-3.95 kPa, which matches the experimentally defined suction-hole pressure range of 0.77-2.67 kPa.

Using the same tracing method, the inlet pressure ranges for broomcorn millet and rapeseed were obtained as 2.37-4.22 kPa and 2.23-4.16 kPa, respectively. These results establish a quantitative mapping between chamber inlet pressure and suction-hole pressure, thereby providing a direct basis for subsequent optimization of the seed metering plate.

Table 3

Relationship between air chamber inlet pressure and suction hole pressure

Item	Millet	Broomcorn millet	Rapeseed
Median suction hole diameter [mm]	0.8	1.2	1.0
Suction hole negative pressure range [kPa]	0.77-2.67	0.97-3.25	0.92-2.81
Air chamber suction inlet negative pressure range [kPa]	2.11-3.95	2.37-4.22	2.23-4.16

Experimental design for seed metering plate optimization

To determine the appropriate combination of suction hole diameter, suction hole thickness, and air chamber inlet negative pressure for different seed types, the factor ranges were defined based on the preliminary single-factor experiments and CFD simulation results. Using millet as an example, the selected ranges were 2.0–4.0 kPa for inlet negative pressure, 0.6–1.0 mm for suction hole diameter, and 0.3–0.7 mm for suction hole thickness.

A three-factor, three-level Box–Behnken response-surface design was employed, and the coded factor levels are listed in Table 4. The experimental design matrix and corresponding results are presented in Table 5. The design with 17 runs was employed, including five center-point replicates to estimate pure error. For each parameter combination, pressure values were extracted at 100 suction-hole positions along the metering plate, and the percentage of qualified pressure values was calculated as the response.

Table 4

Factor levels used in the experimental design

Code	Inlet negative pressure (X_1) [kPa]	Suction hole diameter (X_2) [mm]	Suction hole thickness (X_3) [mm]
-1	2	0.6	0.3
0	3	0.8	0.5
1	4	1.0	0.7

The qualification rate of suction-hole pressure was selected as the response variable. For millet, the acceptable suction-hole pressure range was defined as 0.8-2.7 kPa. Analysis of variance and response-surface optimization were performed in Design-Expert 8.0.6. In the statistical interpretation, the main sources of experimental error considered were seed-size variability after grading, pressure-setting resolution, and repeated positioning differences during testing.

Table 5

Experimental design matrix and results

No.	X_1	X_2	X_3	Y_1 [%]
1	-1	-1	0	74
2	1	-1	0	92
3	-1	1	0	70
4	1	1	0	76
5	-1	0	-1	81
6	1	0	-1	93
7	-1	0	1	72
8	1	0	1	80
9	0	-1	-1	93
10	0	1	-1	82
11	0	-1	1	88
12	0	1	1	78
13	0	0	0	97
14	0	0	0	94
15	0	0	0	89
16	0	0	0	90
17	0	0	0	95

RESULTS AND DISCUSSION

Regression modeling and analysis of variance

Based on the experimental results, a quadratic regression model was established using Design-Expert 8.0.6, with the pressure qualification rate at the suction hole (Y_1) as the response variable and the coded factors (X_1, X_2, X_3) as independent variables:

$$Y_1 = 93 + 5.5X_1 - 5.12X_2 - 3.88X_3 - 3X_1X_2 - X_1X_3 + 0.25X_2X_3 - 9.38X_1^2 - 5.63X_2^2 - 2.12X_3^2 \quad (2)$$

Analysis of variance (ANOVA) was performed to evaluate the significance of the regression model, as summarized in Table 6. The results indicate that the model is statistically significant ($p < 0.05$), while the lack-of-fit term is not significant ($p > 0.05$), confirming that the model adequately describes the experimental data.

Table 6

Analysis of variance (ANOVA) for the regression model

Sources	Sum of squares	Degree of freedom	Mean square	*F*	*p*
Model	1177.69	9	130.85	13.23	0.0013
X_1	242.00	1	242.00	24.46	0.0017
X_2	210.13	1	210.13	21.24	0.0025
X_3	120.13	1	120.13	12.14	0.0102
X_1X_2	36.0000	1	36.0000	3.6390	0.0981
X_1X_3	4.0000	1	4.0000	0.4043	0.5451

Sources	Sum of squares	Degree of freedom	Mean square	*F*	*p*
X_2X_3	0.2500	1	0.2500	0.0253	0.8782
X_1^2	370.0658	1	370.0658	37.4074	0.0005
X_2^2	133.2237	1	133.2237	13.4667	0.0080
X_3^2	19.0132	1	19.0132	1.9219	0.2082
Lack of fit	23.25	3	7.75	0.67	0.6116
Pure error	46	4	11.50		
Total	1246.94	16			

Among the factors, X_1 (inlet negative pressure), X_2 (suction hole diameter), X_3 (suction hole thickness), as well as the quadratic terms X_1^2 and X_2^2, show significant effects on the response ($p < 0.05$). In contrast, the interaction terms are not significant, indicating weak coupling effects among the factors.

Effect of factors and response surface analysis

The effects of the factors on the pressure qualification rate are illustrated in Fig. 5. Among the three variables, inlet negative pressure exerted the strongest influence on the response, followed by suction-hole diameter, whereas suction-hole thickness showed a smaller but still significant main effect. The curved surface in Fig. 5(a) indicates that the qualified rate can be maximized only within a moderate pressure-diameter window; excessively low inlet pressure leads to insufficient suction-hole pressure, whereas excessive inlet pressure increases the risk of over-adsorption.

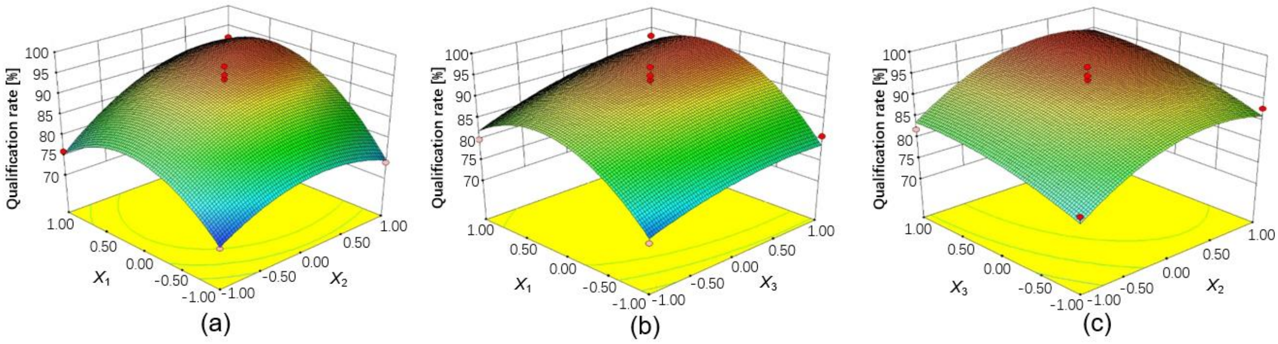

Fig. 5 - Response surfaces to influences of different factors on qualified rate of pressure at the suction hole

(a) X_1 and X_2; (b) X_1 and X_3; (c) X_2 and X_3

As shown in Fig. 5, the qualified rate first increased and then decreased with increasing inlet negative pressure. This trend reflects the transition from insufficient adsorption to an over-strong pressure field. A similar non-monotonic pattern was observed for suction-hole diameter: when the hole was too small, pressure transfer was insufficient, whereas an excessively large hole caused the local pressure to move outside the qualified range. By contrast, increasing suction-hole thickness tended to reduce the qualified rate because the longer flow passage increased local pressure loss and weakened effective pressure transmission near the hole exit.

Parameter optimization and engineering interpretation

Based on the regression model, the optimal parameter combination for millet was an inlet negative pressure of 2.51 kPa, a suction-hole diameter of 0.88 mm, and a suction-hole thickness of 0.31 mm.

Separate Box–Behnken designs were conducted for the three seed types, and only the millet design matrix is shown here as a representative example due to space limitations; the optimized results for the other two seed types are summarized in Table 7. Using the same methodology, the optimal combinations for broomcorn millet and rapeseed were determined to be 2.97 kPa, 1.12 mm, and 0.35 mm, and 2.35 kPa, 0.93 mm, and 0.32 mm, respectively.

The results further confirm that the empirical relationship between seed size and suction-hole diameter, namely that the hole diameter should be approximately 0.4-0.6 times the equivalent seed diameter, is applicable to the present metering system.

Table 7

Optimal parameter combinations for different seed types

Seed type	Inlet negative pressure [kPa]	Suction hole diameter [mm]	Suction hole thickness [mm]
Millet	2.51	0.88	0.31
Broomcorn millet	2.97	1.12	0.35
Rapeseed	2.35	0.93	0.32

Test bench validation experiment

To verify the rationality of the optimized parameter combinations and reduce the influence of random experimental error, a validation bench was established, as shown in Fig. 6. The test bench mainly consisted of a negative-pressure fan, the seed metering device, a high-speed camera, a seed bed belt, and an oil pump. The validation was carried out without seed-cleaning operations so that the filling performance of the seed metering plate itself could be evaluated independently.

According to the optimal simulation results, the parameter combination for millet was a negative pressure of 2.5 kPa, a suction hole diameter of 0.9 mm, and a suction hole thickness of 0.3 mm; for broomcorn millet, the optimal parameters were 3.0 kPa, 1.1 mm, and 0.4 mm, respectively; and for rapeseed, they were 2.4 kPa, 0.9 mm, and 0.3 mm, respectively.

Under the optimized parameter combinations, 100-hole validation tests were conducted for millet, broomcorn millet, and rapeseed. The seed-filling rates reached 93.0 ± 1.4%, 97.0 ± 0.9%, and 96.0 ± 1.1%, respectively. These results indicate that the CFD-based pressure tracing and response-surface optimization provided parameter combinations sufficiently close to the experimental optimum, and therefore can be used as an efficient preselection method for subsequent metering-plate design.

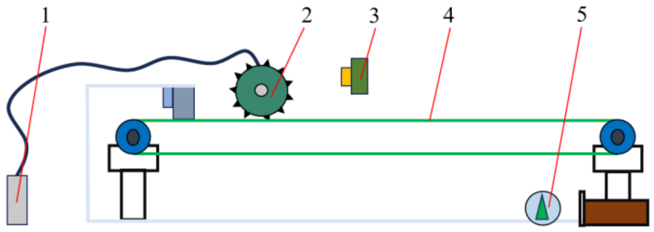

Fig. 6 - Schematic diagram of the seed metering performance test bench

1. negative pressure fan; 2. seed metering device; 3. high-speed camera; 4. seed bed belt; 5. oil pump

CONCLUSIONS

This study systematically investigated the key parameters affecting the performance of a pneumatic seed metering plate for small-seed crops through a combination of experiments, CFD simulation, and optimization analysis. The main conclusions are as follows:

(1) Single-factor tests established the engineering matching relationship between suction-hole diameter and seed size for the present metering system, namely that the suitable suction-hole diameter was 0.4-0.6 times the equivalent seed diameter.

(2) Brushing-threshold experiments and the dedicated adsorption test platform determined the acceptable suction-hole negative-pressure ranges for millet, broomcorn millet, and rapeseed as 0.77-2.67 kPa, 0.97-3.25 kPa, and 0.92-2.81 kPa, respectively.

(3) CFD pressure-tracing analysis clarified the mapping between suction-hole pressure and chamber inlet negative pressure, thereby converting the experimentally defined adsorption range into a directly usable chamber-pressure range for design and adjustment.

(4) Response-surface optimization identified the optimal parameter combinations for the three seed types, and bench validation produced seed-filling rates of 93%, 97%, and 96%, confirming the reliability of the optimized results.

From an engineering perspective, the proposed workflow can be used to narrow the parameter-search space of pneumatic seed metering plates for small-seed crops and reduce repeated physical trials. However, the CFD model was based on a steady and symmetric airflow field and did not explicitly account for transient leakage, plate rotation, or gas-solid coupling with moving seeds. These factors should be incorporated in future transient CFD-DEM studies to further improve predictive accuracy.

ACKNOWLEDGEMENT

This study was supported by the National Natural Science Foundation of China (32272001), the Shaanxi Key Research and Development Project (2023-ZDLNY-62), and the Shaanxi Key Research and Development Project (grant number 2022NY-205).

REFERENCES

[1] Bustos-Gaytán A., Saldaña-Robles N., Joya-Cárdenas D.R., Gutiérrez-Vaca C., Alfaro-Ayala J.A., Barco-Burgos J., & Saldaña-Robles A. (2025). Advancements in pneumatic seed-metering devices: A review of numerical and experimental approaches. *Results in Engineering*, 26, 105626. https://doi.org/10.1016/j.rineng.2025.105626

[2] Cao Z., Yi S., Wang S., Chen T., & Li Y. (2026). Detection method of hole formation in foxtail millet based on K-value (基于 K 值法的谷子穴播成穴性检测方法). *Transactions of the Chinese Society for Agricultural Machinery*, 57(6), 119-128. https://doi.org/10.6041/j.issn.1000-1298.2026.06.011

[3] Cong J., Liao Q., Cao X., Liao Y., Yu J., & Wang L. (2014). Seed filling performance of dual-purpose seed plate in metering device for both rapeseed & wheat seed (油菜小麦兼用排种盘的排种器充种性能). *Transactions of the Chinese Society of Agricultural Engineering*, 30(8), 30-39. https://doi.org/10.3969/j.issn.1002-6819.2014.08.004

[4] Ding L., Yang L., Liu S., Yan B., He X., & Zhang D. (2018). Design of air suction high speed precision maize seed metering device with assistant seed filling plate (辅助充种种盘玉米气吸式高速精量排种器设计). *Transactions of the Chinese Society of Agricultural Engineering*, 34(22), 1-11. https://doi.org/10.11975/j.issn.1002-6819.2018.22.001

[5] Dun G., Yu C., Yang Y., Ye J., Du J., & Zhang J. (2019). Parameter simulation optimization and experiment of seed plate type hole for soybean breeding (大豆育种排种盘型孔参数仿真优化与试验). *Transactions of the Chinese Society of Agricultural Engineering*, 35(19), 62-73. https://doi.org/10.11975/j.issn.1002-6819.2019.19.008

[6] Gaikwad B.B., & Sirohi N.P.S. (2008). Design of a low-cost pneumatic seeder for nursery plug trays. Biosystems Engineering, 99(3), 322-329. https://doi.org/10.1016/j.biosystemseng.2007.10.017

[7] Gao L., Shi B., Liao Q., Zhang B., Zheng J., & Liao Y. (2022). Seeding performance of conical-hole seeding plate of the positive and negative pressure combination precision seed metering device for rapeseed (正负气压组合油菜精量排种器锥孔盘排种性能). *Transactions of the Chinese Society of Agricultural Engineering*, 38(6), 22-33. https://doi.org/10.11975/j.issn.1002-6819.2022.06.003

[8] Gao X., Zhao P., Li J., Xu Y., Huang Y., & Wang L. (2022). Design and experiment of quantitative seed feeding wheel of air-assisted high-speed precision seed metering device. *Agriculture*, 12(11), 1951. https://doi.org/10.3390/agriculture12111951

[9] Hu M., Zhang J., Chen Y., Xu C., & Li, B. (2025). Parameter optimization and experiment of an inside-filling pneumatic high-speed precision seed-metering device for cotton. *INMATEH Agricultural Engineering*, 76(2), 1334-1351. https://doi.org/10.35633/inmateh-76-111

[10] Ibrahim E.J., Liao Q., Wang L., Liao Y., & Yao L. (2018). Design and experiment of multi-row pneumatic precision metering device for rapeseed. *International Journal of Agricultural and Biological Engineering*, 11(5), 116-123. https://doi.org/10.25165/j.ijabe.20181105.3544

[11] Karayel D., Barut Z.B., & Ozmerzi A. (2004). Mathematical modelling of vacuum pressure on a precision seeder. *Biosystems Engineering*, 87(4), 437-444. https://doi.org/10.1016/j.biosystemseng.2004.01.011

[12] Karayel D., Barut Z.B., & Özmerzi A. (2022). Estimation of optimum vacuum pressure of air-suction seed-metering device of precision seeders using artificial neural network models. *Agronomy*, 12(7), 1600. https://doi.org/10.3390/agronomy12071600

[13] Li X., Liao Q., Wang L., Li M., & Du W. (2023). Design and experiments of the type-hole wheel with high-speed air-assisted centralized metering device for rice, wheat and rapeseed (稻麦油兼用高速气送式集排器型孔轮设计与试验). *Transactions of the Chinese Society of Agricultural Engineering*, 39(14), 35-48. https://doi.org/10.11975/j.issn.1002-6819.202303044

[14] Li Z., Yang W., Zhang T., Wang W., Zhang S., & Chen Li. (2019). Design and suction performance test of sucking-seed plate combined with groove-tooth structure on high speed precision metering device of rapeseed (油菜高速精量排种器槽齿组合式排种盘设计与吸附性能试验). *Transactions of the Chinese Society of Agricultural Engineering*, 35(1), 12-22. https://doi.org/10.11975/j.issn.1002-6819.2019.01.002

[15] Liao Y., Wang L., & Liao Q. (2017). Design and test of an inside-filling pneumatic precision centralized seed-metering device for rapeseed. *International Journal of Agricultural and Biological Engineering*, 10(2), 56–62, https://doi.org/10.3965/j.ijabe.20171002.2061

[16] Liu D., Ma J., Qiao X., Xin P., Zhang X., Wang J., & Zheng D. (2023). The design of and experiments with a double-row seed-metering device for buckwheat breeding in an experimental area. *Agronomy*, 13(12), 2857. https://doi.org/10.3390/agronomy13122857

[17] Onal I., Degirmencioglu A., & Yazgi A. (2012). An evaluation of seed spacing accuracy of a vacuum type precision metering unit based on theoretical considerations and experiments. *Turkish Journal of Agriculture and Forestry*, 36(2), 133-144. https://doi.org/10.3906/tar-1010-1316

[18] Panning J.W., Kocher M.F., Smith J.A., & Kachman S.D. (2000). Laboratory and field testing of seed spacing uniformity for sugarbeet planters. *Applied Engineering in Agriculture*, 16(1), 7-13. https://doi.org/10.13031/2013.4985

[19] Ren D., Liu Tao, Xia S., Chen Y., Wang W., & Li Z. (2024). Design and seed filling performance test of cavity plate combination hole type seeding plate for corn and soybean (玉米大豆兼用腔盘组合孔式排种盘设计与充种性能试验). *Transactions of the Chinese Society for Agricultural Machinery*, 55(2), 73-89. https://doi.org/10.6041/j.issn.1000-1298.2024.02.007

[20] Rezaei Asl A., Roudbari M., & Esmailzadeh E. (2019). Fabrication and evaluation of vacuumed metering drum performance for row planting of soybean with grease belt. *Agricultural Engineering International: CIGR Journal*, 21(4), 96-106.

[21] Shi Y., Zhang X., Yan J., Ma X., Li H., & Han C. (2025). Calibration and optimization of discrete element parameters for tiger nuts. *INMATEH Agricultural Engineering*, 76(2), 978-993. https://doi.org/10.35633/inmateh-76-84

[22] Singh R.C., Singh G., & Saraswat D.C. (2005). Optimisation of design and operational parameters of a pneumatic seed metering device for planting cottonseeds. *Biosystems Engineering*, 92(4), 429-438. https://doi.org/10.1016/j.biosystemseng.2005.07.002

[23] Tang H., Xu F., Xu C., Zhao J., & Wang Y. (2023). The influence of a seed drop tube of the inside-filling air-blowing precision seed-metering device on seeding quality. *Computers and Electronics in Agriculture*, 204, 107555. https://doi.org/10.1016/j.compag.2022.107555

[24] Wang B., Liao Q., Wang L., Shu C., Cao M., & Du W. (2023). Design and test of air-assisted seed-guiding device of precision hill-seeding centralized seed-metering device for sesame. *Agriculture*, 13(2), 393. https://doi.org/10.3390/agriculture13020393

[25] Wang B., Wang Z., Luo X., Zhang M., Fang L., Liu S., & Xu P. (2019). Design and experiment of wedge churning device for pneumatic cylinder-type seed metering device for hybrid rice (杂交稻气力滚筒集排式排种器楔形搅种装置设计与试验). *Transactions of the Chinese Society of Agricultural Engineering*, 35(23), 1-8. https://doi.org/10.11975/j.issn.1002-6819.2019.23.001

[26] Wang F., Lv B., Wang H., & Zhao M. (2017). Structural design and test of seed-suction hole of air-sucking seed-metering device for millet (气吸式谷子排种装置吸种孔的结构设计与试验). *Transactions of the Chinese Society of Agricultural Engineering*, 33(8), 30-36. https://doi.org/10.11975/j.issn.1002-6819.2017.08.004

[27] Wei S., Ding Y., Dong W., Liao Q., Wang S., Nong F., & Huang Q. (2026). Design and experiment of precision pneumatic seed metering device with adjustable seeds per hole for cotton (穴粒数可调气吸式棉花精量排种器设计与试验). *Transactions of the Chinese Society for Agricultural Machinery*, 57(2), 32-45. https://doi.org/10.6041/j.issn.1000-1298.2026.02.004

[28] Xing H., Zhang G., Han Y., Gao Y., & Zha X. (2020). Development and experiment of double cavity pneumatic rice precision direct seeder (双腔气力式水稻精量水田直播机设计与试验). *Transactions of the Chinese Society of Agricultural Engineering*, 36(24), 29-37. https://doi.org/10.11975/j.issn.1002-6819.2020.24.004

[29] Yang R., He Y., Chen D., Chen L., Li G., & Zha X. (2026). Design and experiment of air-suction double disc combined maize plot seed meter (气吸双盘组合式玉米小区排种器设计与试验). *Transactions of the Chinese Society for Agricultural Machinery*, 57(6), 67-77. https://doi.org/10.6041/j.issn.1000-1298.2026.06.007

[30] Yazgi A., & Degirmencioglu A. (2007). Optimisation of the seed spacing uniformity performance of a vacuum-type precision seeder using response surface methodology. *Biosystems Engineering*, 97(3), 347-356. https://doi.org/10.1016/j.biosystemseng.2007.03.013

[31] Yu J., Liao Y., Cong J., Yang S., & Liao Q. (2014). Simulation analysis and match experiment on negative and positive pressures of pneumatic precision metering device for rapeseed. *International Journal of Agricultural and Biological Engineering*, 7(3), 1-12. https://doi.org/10.3965/j.ijabe.20140703.001

[32] Zhang X., Wen Z., Wang Q., Li H., Zhang Z., & Liu J. (2022). Research on characteristics of airway pressure loss in seeding-wheel-type pneumatic seeder. *Agriculture*, 12(12), 2021. https://doi.org/10.3390/agriculture12122021

[33] Zhao X., Zhang T., Liu F., Li N., & Li J. (2023). Sunflower seed suction stability regulation and seeding performance experiments. *Agronomy*, 13(1), 54. https://doi.org/10.3390/agronomy13010054

[34] Zhong W., Zhao X., Liu F., Bai H., Dong W., Hu H., & Kong X. (2024). Design and experiment of precision seed metering device for flow adsorption of quinoa seeds. *Agriculture*, 14(3), 434. https://doi.org/10.3390/agriculture14030434